Available online at www.sciencedirect.com
ScienceDirect
Ceramics International 36 (2010) 2315–2321
CERAMICS INTERNATIONAL
www.elsevier.com/locate/ceramint

An in situ high pressure-high temperature powder diffraction study of the formation of a precursor phase of bismuth manganite

R.J. Cernik [a,*], Leonid Dubrovinsky [b], R. Freer [a], M. Thrall [a]

[a] Materials Science Centre, School of Materials, University of Manchester, Grosvenor Street, Manchester M1 7HS, UK
[b] Bayerisches Geoinstitut, Universität Bayreuth, D-95440 Bayreuth, Germany

Received 19 March 2010; received in revised form 8 April 2010; accepted 4 June 2010
Available online 3 August 2010

Abstract

The synthesis route for single phase $BiMnO_3$ from Bi_2O_3 and Mn_2O_3 has been undertaken, in situ, in a diamond anvil cell. The starting powders were mixed in a stoichiometric ratio and loaded into a diamond anvil cell with a gasket aperture of 150 μm. A ruby chip was used to measure the pressure and a circular resistive heater surrounded the central core of the cell. The reaction was studied as a function of pressure and temperature to 6.7 GPa and 480 °C by X-ray diffraction. There was evidence of the onset of a reaction between the starting oxides at 314 °C and 6.7 GPa but there was no evidence of transformation of the monoclinic Bi_2O_3 to the cubic form before the reaction began. A monoclinic phase related to the structure of multiferroic $BiMnO_3$ was observed to form with space group Cc, $a = 10.21(1)$, $b = 5.356(6)$, $c = 10.38(1)$ Å and $\beta = 116.87(6)^\circ$. A good fit for this structure was obtained by modelling a distorted $BiMnO_2$ unit cell with disordered Bi and Mn sites. We did not go sufficiently high in temperature to observe the formation of single phase $BiMnO_3$ but the precursor phase was observed to persist when returned to room temperature and pressure.

Keywords: A: Powders: solid state reactions; B: X-ray methods; E. Functional applications

1. Introduction

Multiferroics are materials which exhibit simultaneously at least two characteristic behaviour types from ferroelectric, ferromagnetic or ferroelastic. Interest in these materials as sensors, actuators and storage devices has grown in recent years but there has been a practical difficulty in maximising the coupling between ferroic parameters. This has been partially addressed by work on thin films, particularly $BiFeO_3$, enabling control of multiferroic properties by epitaxial strain and strain gradients [1].

By analogy with $BiFeO_3$ it was anticipated that $BiMnO_3$ might also behave as a multiferroic. It was postulated that bulk $BiMnO_3$ has a ferroelectric Curie temperature of ∼450 K [2] and demonstrated that $BiMnO_3$ has ferromagnetic ordering below ∼100 K with a large magnetisation per formula unit [3,4]. Hill and Rabe [5] proposed that by introducing rare earth (R) atoms into bismuth manganite the covalent bonding between bismuth cations and oxygen anions would be complemented by another purely ionic interaction between the rare earth and oxygen. They argued that these additional orbital interactions would stabilize different magnetic and structural phases and that the rare earth-based manganites ($RMnO_3$) might yield materials with useful multiferroic properties. Subsequently Kimura et al. [6] indicated how ferroelectric polarisation could be controlled in $TbMnO_3$. The manganites $HoMnO_3$ and $YMnO_3$ were also shown to be multiferroic.

A serious problem in the development of high quality multiferrioics has been the preparation of pure, single phase materials. Some success had been achieved with single crystals and float zone methods but it was not until 2007 that Belik et al. [7] demonstrated that pure $BiMnO_3$ could be synthesised at high pressure. Detailed structural determinations, for $BiMnO_3$ synthesised in different ways, have appeared over the past decade. Atou et al. [8] using electron diffraction and neutron diffraction proposed a monoclinic space group (C2) for material synthesised at high pressure. Yokosawa et al. [9] also

* Corresponding author.
E-mail address: b.Cernik@manchester.ac.uk (R.J. Cernik).

0272-8842/$36.00
doi:10.1016/j.ceramint.2010.07.014

used electron diffraction and suggested that the space group for $BiMnO_3$ could be assigned to C2/c. However, they found evidence of non-centrosymmetric long-range order (related to space group C2) and suggested there was correlation between the Bi^{3+} and Mn^{3+} ions. The role of oxygen non-stoichiometry in defining the structure of $BiMnO_3$ was highlighted by Sundaresan et al. [10]. Belik et al. have undertaken a series of investigations [11,12] to define the structure and understand the structural control of multiferroic properties in $BiMnO_3$. They also found that it was not possible to synthesis oxygen non-stoichiometric $BiMnO_3$ by direct high pressure routes, and that alternative strategies were required [13]. Materials with monoclinic and orthorhombic structures were obtained at different levels of non-stoichiometry. In high pressure studies of $BiMnO_3$ at ambient temperature, Belik et al. [13] proposed a new monoclinic phase having P2(1)/c symmetry between 1.5 and 5.5 GPa, whilst above 8 GPa, the orthorhombic GdFeO3-type phase (space group Pnma) was stable. More recently Toulemonde et al. [14] have reported an intermediate phase before the development of the orthorhombic and monoclinic phases but the crystal structure of this phase was not solved.

We have undertaken an in situ high pressure, high temperature X-ray diffraction investigation to examine the reaction between the constituent oxides (Bi_2O_3 and Mn_2O_3) and to examine the intermediate phase in more detail. The study will contribute to the understanding of the conditions leading to the formation of single phase $BiMnO_3$.

2. Experimental procedures

The starting powders of Bi_2O_3 (≥98% purity) and Mn_2O_3 (≥99% purity) were mixed (1:1 ratio Bi_2O_3:Mn_2O_3) with propanol-2 and zirconia media in a polythene flask by vibro-milling for 16 h. The powders were dried at 100 °C for 4 h to remove any organic species.

The in situ, X-ray powder diffraction investigations of the sintering cycle of $BiMnO_3$ were undertaken at the Bavarian Geological Institute (University of Bayreuth, Germany), utilising a modified Merrill-Basset type design Diamond Anvil Cell (DAC), with diamonds of 300 μm cutlet size. The mixed powders (without any pressure medium) were loaded into a Re gasket that had been pre-indented to ∼30 μm and then drilled to produce a hole of 150 μm. For pressure calibration small ruby chips were loaded into the pressure cell with the sample powder; calibration was based on the ruby R_2 fluorescence peak position [15]. Specimen heating was provided by resistive heating coils, mounted concentrically with the DAC (Fig. 1). X-rays were produced by a FRD high brilliance molybdenum rotating anode generator. The Mo Kα radiation (λ = 0.7108A) was collimated to approximately 50 μm diameter (full width at half maximum height) beam size and aligned with the hole in the rhenium gasket. The scattered X-rays were collected in transmission geometry through the DAC on an APEX CCD area detector. The Debye–Scherrer rings were circularly integrated to produce a one-dimensional powder diffraction pattern using FIT2D software [16]. Any spots caused by abnormally large grains were removed manually using the same software.

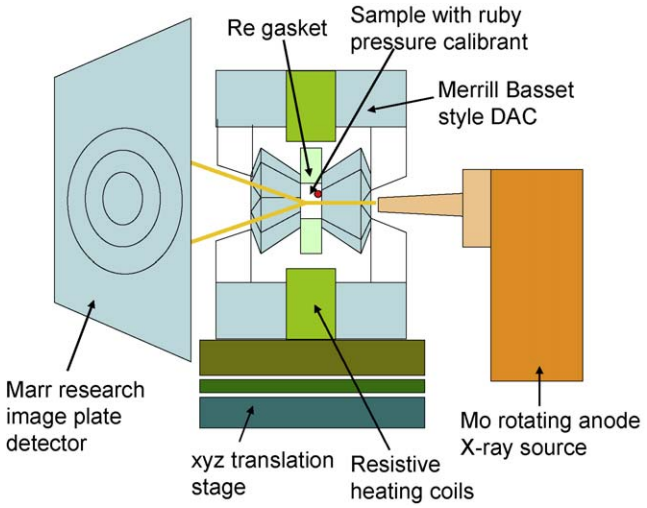

Fig. 1. Experimental arrangement employed for investigating the reacting oxides as a function of pressure and temperature; the image plate is offset for clarity.

Before heat was applied, the pressure in the diamond anvil cell was increased approximately uniformly (over a period of 7 h) to a maximum of 6.7 GPa. It was then left at this pressure for 15 h to allow the system to stabilise. The temperature was then raised slowly to a maximum of 480 °C, with holds of between 15 and 60 min (depending on scattering efficiency) at intermediate temperatures to allow data collection. After annealing for 15 h at the maximum temperature and pressure, data were collected again to assess the stability of the material produced. The temperature was then reduced to ambient, and finally the pressure was reduced to atmospheric. Data sets were also collected during the initial pressurising cycle, and after reducing temperature and then pressure. In total 16 data sets were collected as the temperature varied from ambient to 480 °C; the pressure was varied from ambient to a maximum of 6.7 GPa. This approach produced refineable data for a 2θ range of 20° for each set of conditions. All 16 processed diffraction patterns were refined by the multiphase Rietveld method using TOPAS [17] which is a fast and stable nonlinear least squares Rietveld refinement program. The starting structures for all phases were obtained from the chemical data service databank operated by Daresbury Laboratory [18]

3. Results and discussion

In the first phase of the experiment, the sample cell was held at ambient temperature and the pressure increased, in approximately uniform steps, to 6.7 GPa. X-ray diffraction data sets were collected in six steps during pressurising. One-dimensional X-ray powder diffraction patterns were reconstructed by circular integration of the Debye–Scherrer rings for each set of conditions. The only effects observed with increasing pressure were decreasing lattice parameters and peak broadening due to strain. However, there was no evidence of a change in structure caused solely by the increasing

pressure. All the data sets were analysed by Rietveld refinement of the powder profiles using TOPAS as described above. Fig. 2 shows the refined data for ambient temperature and 2 GPa. The uppermost line shows the observed data; superimposed on it is the calculated fit; the two lines are almost indistinguishable. The difference between the observed and calculated lines is shown by the lowest (feint) line on the figure. The phase percentages calculated from the scale factors from the Rietveld analysis were 76(±3)% Bi_2O_3:24(±3)% Mn_2O_3. Within the accuracy of the method this is equivalent to a 1:1 stoichiometric ratio.

After stabilising the pressure cell at 6.7 GPa for 15 h, the temperature was increased. Data sets were collected at seven temperatures between ambient and 480 °C. For temperatures up to 300 °C there is little evidence of any reaction, and the refined diffraction data are essentially the same as that shown in Fig. 2 for the starting materials, and hence the phase percentage ratio for Bi_2O_3:Mn_2O_3 was unchanged. Microabsorption did not appear to be a problem, in spite of the large difference in atomic number between Bi and Mn; we attribute this to the relatively uniform and small sizes of the crystallites.

With increasing temperature the reaction between Bi_2O_3 and Mn_2O_3 to form $BiMnO_3$ progressed to completion. Fig. 3 shows three sets of diffraction data as the sample was heated to the maximum temperature. The changes from the starting materials (line 1), to the initial and partial reaction (line 2), to the final product after annealing (line 3) is quite clear. Fig. 4 shows the final data set at high temperature and pressure (data points represented by circles) with the Rietveld refined profile. The room temperature and pressure scan is also shown superimposed on the high temperature-high pressure data. It can be seen that the lattice parameter has increased due to the drop in pressure but that no significant structural changes have taken place on cooling and depressurisation. Toulemonde et al. [14] have collected ESRF data at much higher energy (corresponding to our 10–18° 2θ range) and their observed lies are superimposed on our data to show the similarity between the intermediate phase they reported and our observed phase. This is shown on the inset in Fig. 4. It can be seen that there is a good match between the d spacings of the two structures with the exception of a medium strength peak at ~16.5° which we did not observe. The mean value for χ^2 from the Rietveld analysis was 1.3(±0.1) which improved to 1.1(±0.1) after annealing the sample.

Fig. 5 summarises the phase percentages obtained from the quantitative Rietveld refinement of all the data sets. Data sets 1–7 represent the increase in pressure from ambient to 6.7 GPa; there is no significant change in the quantity of the starting oxides or reaction of the starting oxides. Data set 8 was collected at 218 °C and shows no change from the data at ambient temperature data sets 1–7. The onset of the reaction was first apparent at 314 °C (data set 9). There was no change in the structure or the crystalline nature of Bi_2O_3 or Mn_2O_3 before the reaction to form $BiMnO_3$. Data sets 10–14 show an increase in phase percentage of the final product up to a maximum of 92%. There was still evidence of ~2–4% unreacted starting material in the final product. The final two data sets reflect the material as the temperature reduced to ambient temperature at 6.7 GPa (point 15) and finally with both temperature and pressure reduced to ambient (point 16). Table 1 shows the refined cell parameters for precursor $BiMnO_3$ from the initial reaction at 314–480 °C together with the goodness of fit indicators and the errors from the Rietveld output. With the existing data we are not able to specify the stoichiometry of the final product that would require a range in q space and better angular resolution.

In an earlier in situ synchrotron study of the reaction between Bi_2O_3 and Fe_2O_3 to form $BiFeO_3$ at ambient pressure [19] we found that the starting powder Bi_2O_3 transformed fully from the monoclinic form to the cubic form at 650–700 °C before the final reaction to form bismuth ferrite began at

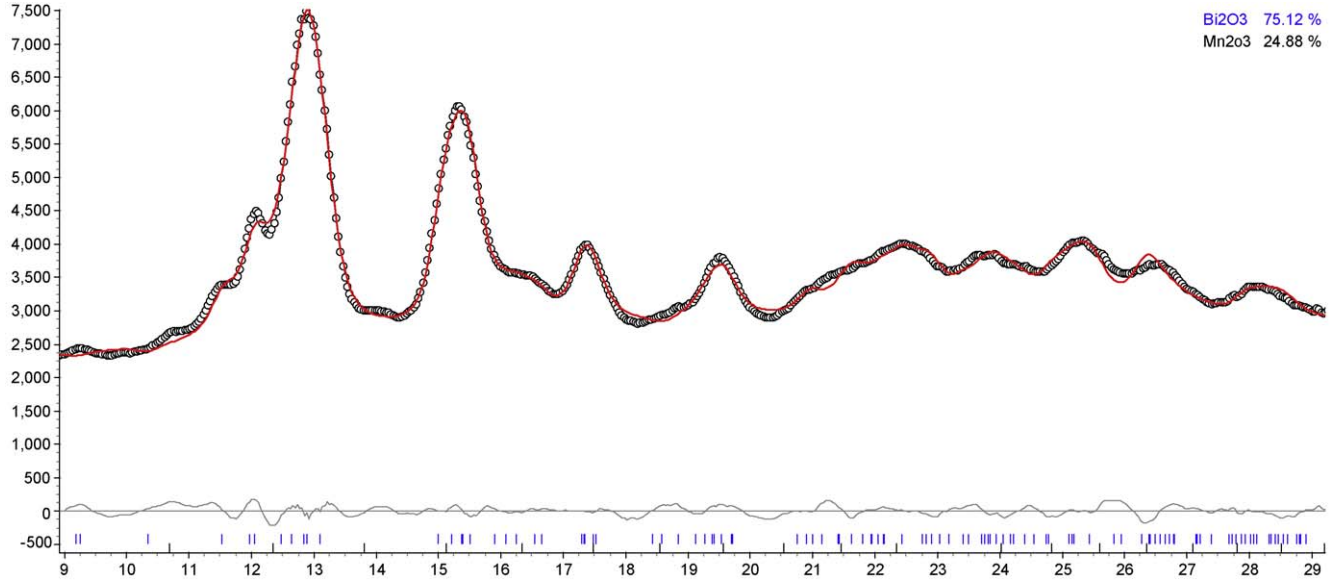

Fig. 2. Rietveld refined X-ray data collected at ambient temperature and 2 GPa: the observed data is shown by the circular data points with the calculated fit by the solid line through the data points; the difference between I_{obs} and I_{calc} is shown by the lower line.

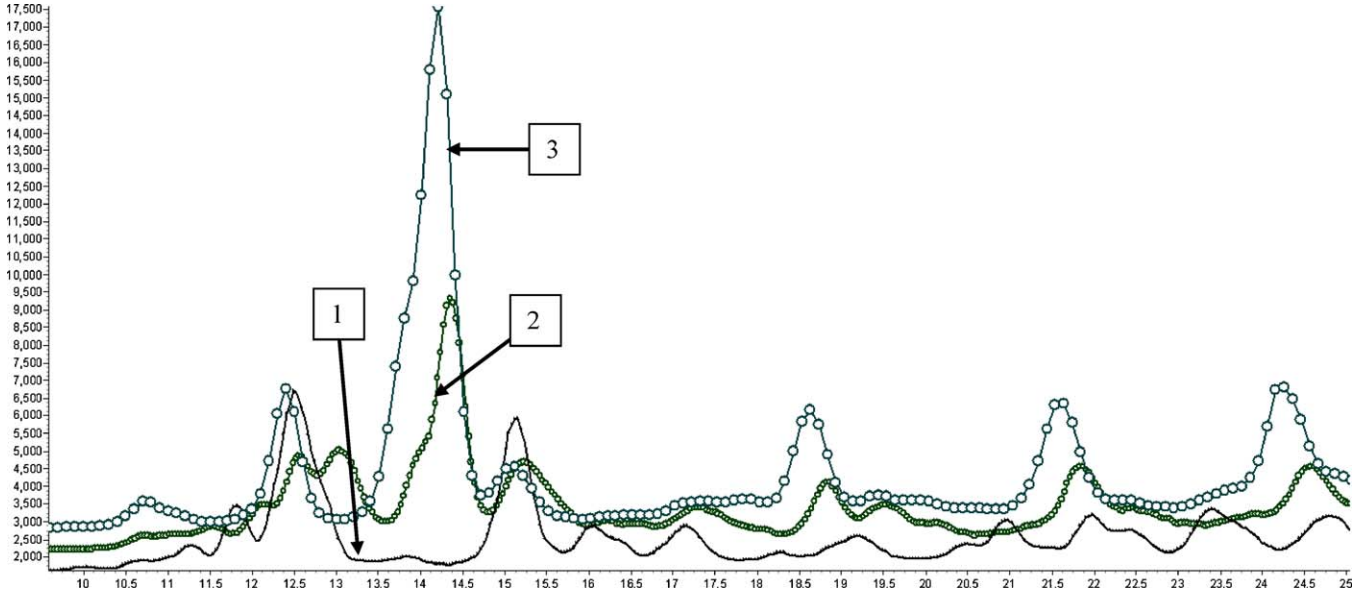

Fig. 3. Three representative X-ray spectra, collected at the beginning, during and after the reaction. Line 1 represents the diffraction spectrum from the initial mixed oxides at ambient temperature and pressure; line 2 shows the spectrum for the start of the reaction at 6.7 GPa and 314 °C; and line 3 shows the spectrum for the final product after cooling from 480 °C and the release of pressure from 6.7 GPa to ambient.

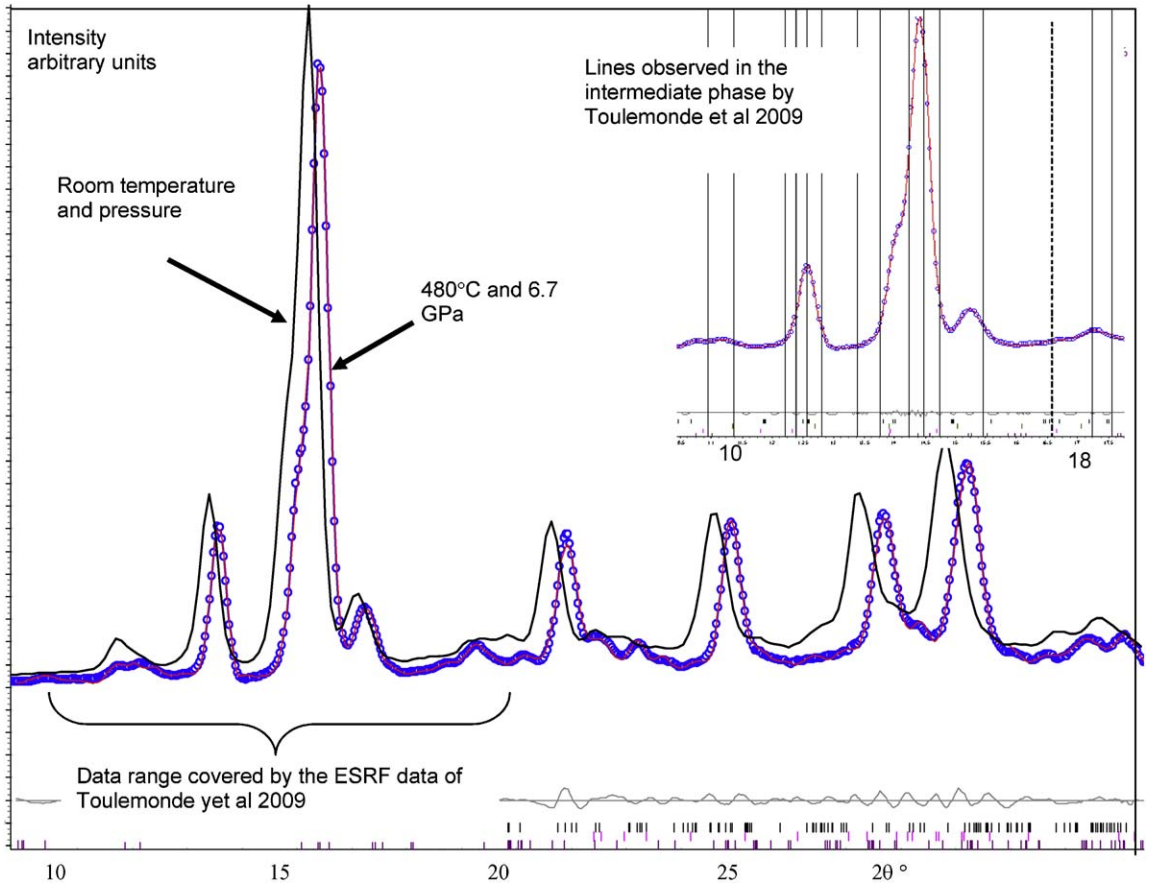

Fig. 4. X-ray diffraction pattern collected 480 °C and 6.7 GPa, the observed data are marked by the circles with the red line showing the calculated fit from the Rietveld refinement. The solid black line shows the diffraction pattern collected at room temperature and pressure from the same material. The refined structure is essentially the same except for an increase in lattice parameter. The inset shows the data from 10° to 18° 2θ with a set of lines that show the observed peaks published by Toulemonde et al. [14], the similarity is clear although the dotted line shows a medium strong peak that we did not observe.

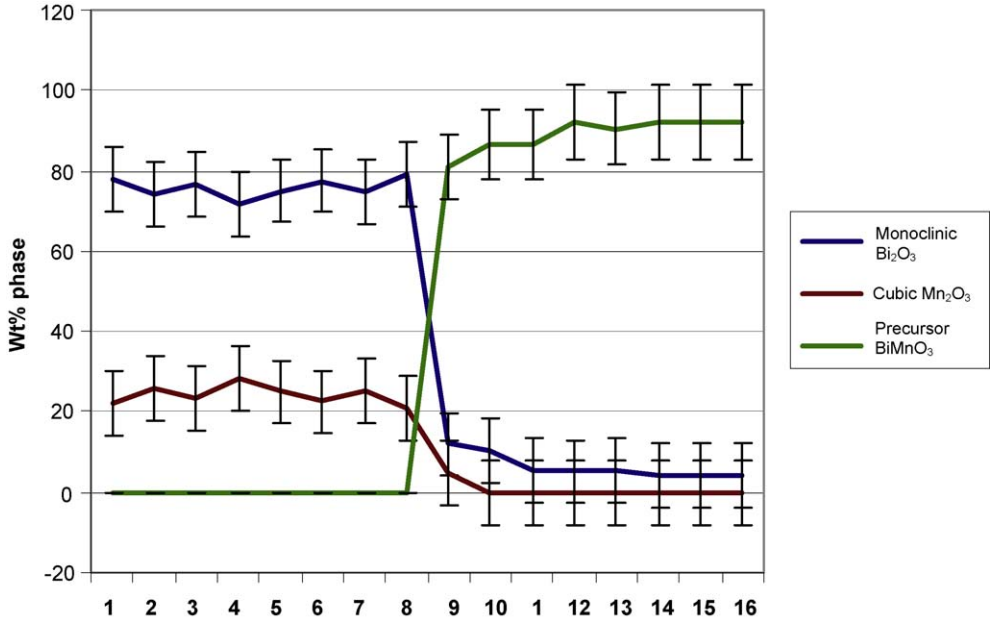

Fig. 5. The phase percentages obtained from quantitative Rietveld refinement of multiple data sets during the reaction of Bi_2O_3 and Mn_2O_3 to form precursor $BiMnO_3$ (pressures up to 6.7 GPa and temperatures up to 480 °C). Points 1–7 represent ambient temperature and pressure rising to 6.7 GPa; points 8–14 are for the temperature increasing at 6.7 GPa; point 15 is for the sample at maximum temperature and pressure after annealing; point 16 is for the sample at ambient temperature and pressure. There is no transformation of Bi_2O_3 to the cubic form before the reaction occurs.

800 °C. In addition Atou et al. [20] saw that the same transition took place at 4.5 GPA above 550 K. In the present study we saw the direct formation of precursor bismuth manganite from the monoclinic form of Bi_2O_3 and cubic Mn_2O_3. Applied pressure gradients [21] in the diamond anvil cell may have an effect on the transformation temperatures, especially since we were unable to work with a pressure equilibrating hydrostatic medium.

We used the space group C2/c for all our refinements; this yielded a satisfactory fit in all cases. However, the study of Belik et al. [11] achieved significantly higher resolution using the Spring8 synchrotron and a much higher X-ray energy (∼38 keV). This gave a much higher resolution in q space and enabled them to identify a series of subtle phase transitions from C2/c through P2(1)/c to Pnma. We have attempted to use these space groups in our refinements but the detail available from the laboratory X-ray data is insufficient, compared with the Spring8 data, to undertake any realistic structural evaluation and comparison. The P2(1)c phase is manifest in X-ray data as very fine peaks on the shoulders of the main cluster. Whilst we were not able to observe the minor peaks and monitor the subtle structural changes, the laboratory data were still of suitable quality to examine the reaction between Bi_2O_3 and Mn_2O_3 as a function of temperature, which was the prime focus of the investigation.

Belik et al. [11] used a belt cell operating at 1383 K and 6 GPa to prepare $BiMnO_3$; no further details of the synthesis were provided. The belt cell is capable of holding much larger samples than a diamond anvil cell and can therefore maintain a more uniform and representative pressure. However, 6.7 GPa is a relatively modest pressure for a diamond anvil cell which allowed us to used a large gasket aperture of 150 μm. We were not able to use a hydrostatic pressure medium as this might have affected the reaction conditions. It has been noted in the past that large pressure gradients can build up in diamond anvil cells without such a pressure equalising medium [17]. However, the ruby chip used for pressure calibration did not show any sharp deviations and the cell was allowed to settle before collecting

Table 1
Refined values of lattice parameter and cell volumes for $BiMnO_3$, with R factors and goodness of fit.

	Rexp %	Rwp %	GoF	Cell vol.	σ (V)	a	b	c	σ (a)	σ (b)	σ (c)
314 °C 6.7 GPa	1.71	2.3	1.34	395.7	0.4	10.040	4.488	9.057	0.007	0.002	0.007
358 °C 6.7 GPa	1.69	3.62	2.14	322.1	1.0	10.196	3.769	8.770	0.027	0.005	0.008
381 °C 6.7 GPa	1.46	3.55	2.44	397.3	1.1	10.262	4.351	9.113	0.019	0.007	0.011
407 °C 6.7 GPa	1.51	2.82	1.87	403.0	2.7	10.441	4.352	9.105	0.063	0.008	0.020
480 °C 6.7 GPa	2.46	4.27	1.73	398.7	0.5	9.980	4.489	9.148	0.007	0.003	0.006
450 °C 6.7 GPa after 15 h annealing	1.53	1.62	1.1	398.5	0.5	10.484	4.319	9.021	0.010	0.002	0.005
Room temp. 19 °C 6.7 GPa	2	3.62	1.81	373.3	0.5	10.098	4.264	8.840	0.009	0.003	0.008
Room temp. 19 °C room pressure 0 GPa	1.32	2.42	1.84	400.1	1.2	10.164	4.385	9.170	0.022	0.004	0.013

Table 2
Refined .site occupancies of the phase formed at 480 °C and 6.7 GPa.

	Site	Np	*x*	*y*	*z*	Atom	Occ.	Beq.
1	Bi1	4	0.1287	0.2186	0.1212	Bi^{3+}	0.88 (9)	0.5
2						Mn^{2+}	0.12 (9)	0.5
3	Bi2	4	0.8563	0.218	0.369	Bi^{3+}	0.84 (8)	0.5
4						Mn^{2+}	0.16 (8)	0.5
5	Mn1	4	−0.009	0.7883	0.25	Mn^{3+}	0.42 (10)	0.5
6						Bi^{3+}	0.58 (10)	0.5
7	Mn2	4	0.25	0.236	0.5	Mn^{3+}	0.55 (10)	0.5
8						Bi^{3+}	0.45 (10)	0.5
9	O3	4	0.1427	0.5789	0.3719	O^{2-}	1	1
10	O4	4	0.8511	0.5634	0.1364	O^{2-}	1	1
11	O5	4	0.347	0.552	0.1624	O^{2-}	1	1
12	O6	4	0.6385	0.5438	0.3338	O^{2-}	1	1

data. It is therefore unlikely that the observed formation temperature for $BiMnO_3$ was significantly depressed by a local non-hydrostatic pressure increase giving rise to an anomalously high local pressure. We can speculate that the use of higher pressures could be useful in synthesising $BiMnO_3$ because of lower transition temperatures. In order to confirm this, a more detailed synchrotron study, including the exploration of temperature and pressure gradients, would be desirable.

Despite these experimental problems we have been able to model a structure that fits the observed phase with an overall goodness of fit χ^2 of 1.8 as shown in Fig. 4. Initially we attempted to fit the C2/c monoclinic structure of $BiMnO_3$ to the data. This would only generate a fit to the data with an unacceptably large distortion of the lattice parameter. The best fit was achieved space group Cc, which is a non-isomorphic sub group of the ordered $BiMnO_3$ parent material. This yielded cell parameters of $a = 10.21(1)$, $b = 5.356(6)$, $c = 10.38(1)$ Å and $\beta = 116.87(6)^\circ$.

There are strong similarities between the monoclinic structure for $BiMnO_3$ reported by Belik et al. [11] and the diffraction patterns of the intermediate phase reported by Toulemonde et al. [14]. The latter group did not formally refine the data for the intermediate phase or postulate a structure, but noted that it was followed at higher temperatures by an orthorhombic phase and then the monoclinic phase reported by Belik et al. [12].

We noticed for the phase formed at 480 °C and 6.7 GPa that there were substantial electron density differences from the stoichiometric 1:1 ratio on all Bi and Mn sites. This leads us to postulate that it might be a disordered variant of the parent structure with shared occupancy of the Bi and Mn sites. The site occupancies were refined as shown in Table 2. The standard deviation for site occupancy averaged 0.3 which, when taken with the refined data gives a very similar value to that for monoclinic $BiMnO_3$. For our material the first two sites are Bi rich and the second two sites (occupied by Mn in the monoclinic phase) have close to 50:50 Bi:Mn ratios. These occupancies give a theoretical density of 9.0(5) g cm^{-3}. If the Bi and Mn sites are disordered in the way indicated by our refined data we would anticipate a significant change in lattice parameter, driven by Jahn–Teller distortions. These distortions would be expected to lower the symmetry of the phase.

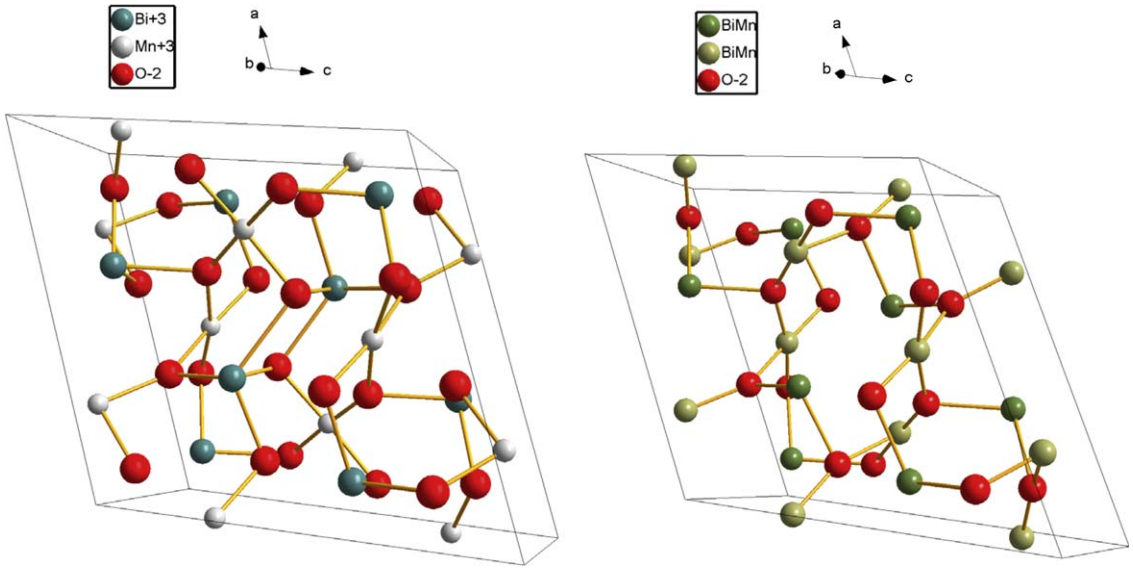

Fig. 6. Structures of (a) ordered $BiMnO_3$ based on the data of Belik et al. [11], and (b) disordered intermediate phase related to $BiMnO_3$. There are significant coordination shifts on three of the four Bi–Mn sites of the intermediate phase (b) with respect to (a).

The proposed structure for the intermediate (precursor) phase is shown in Fig. 6 together with the monoclinic structure reported by Belik et al. [13]. The similarities are clear; the disorder has resulted in significant changes in atomic co-ordination, driving to lower symmetry and expansion of the cell volume. However, the angular resolution of our data is insufficient to detect the subtle changes of structure which are likely to be occurring.

4. Conclusions

We have shown how the starting oxides Bi_2O_3 and Mn_2O_3 react under high pressure and high temperature to yield a precursor to $BiMnO_3$. Unlike perovskite formation in the analogous $BiFeO_3$, there was no transformation of the monoclinic form of Bi_2O_3 to the cubic form before the reaction with Mn_2O_3 was initiated. Both powders retained their original structures. This has not been observed before but may be due to the pressure gradients within the cell creating more thermodynamically stable conditions for the persistence of the monoclinic bismuth oxide form. This is, as yet, not well understood. There was evidence of onset of a reaction by 314 °C and 6.7 GPa (80% complete) and 92% complete by ~350 °C at 6.7 GPa. The X-ray diffraction data collected at 6.7 GPa and ambient pressure are not compatible with the published structures for $BiMnO_3$ but are very similar to data reported by Toulemonde et al. [14] for an unknown intermediate phase. The inset in Fig. 4 shows their data (collected at a wavelength of 0.173 Å at ESRF) superimposed on our data. All peaks correspond with the exception of a medium strong feature at ~16.6° 2θ which we did not observe. This could be either due to preferred orientation differences or structural or space group differences. The problem in resolving these questions lies in the limited range of both data sets. Our data refined much more naturally in the space group Cc, which is a non-isomorphic sub group of the ordered $BiMnO_3$ parent material. The disordered crystal structure we propose for the intermediate phase refined to a slightly better goodness of fit with lower occupancies of bismuth on both sites, however this is not statistically significant. This could explain the presence of small quantities of unreacted bismuth oxide present with the intermediate phase.

The intermediate phase persisted when the pressure and temperature were reduced to ambient conditions indicating that this phase is, at least, metastable. We originally planned to raise the temperature further to create single phase $BiMnO_3$ but were prevented from doing so by experimental limitations. We plan a high energy synchrotron radiation experiment in the near future to collect a wider range of higher resolution data to test the structural details we have proposed here since neither our data range nor quality can unambiguously determine the space group or site occupancies.

Acknowledgements

We gratefully acknowledge the support of the Bavarian Geological Institute (University of Bayreuth, Germany) under the auspices of the EU seventh framework programme and the EPSRC for support via award GR/T19148.

References

[1] R. Ramesh, N. Spaldin, Multiferroics progress and prospects in thin films, Nat. Mater. 6 (2007) 21–29.
[2] A. Moreira dos Santos, S. Parashar, A.R. Raju, A.K. Cheetham, C.N.R. Rao, Evidence for the occurrence of magnetoferroelectricity in $BiMnO_3$, Solid State Commun. 122 (2002) 49–52.
[3] H. Chiba, T. Atou, Y. Syono, Magnetic and electrical properties of Bi $1-x$ Srx MnO_3: hole-doping effect on ferromagnetic perovskite $BiMnO_3$, J. Solid State Chem. 132 (1) (1997) 139–143.
[4] E. Montanari, L. Righi, G. Calestani, A. Migliori, E. Gilioli, F. Bolzoni, Room temperature polymorphism in metastable $BiMnO_3$ prepared by high-pressure synthesis, Chem. Mater. 17 (7) (2005) 1765–1773.
[5] N.A. Hill, K.M. Rabe, First-principles investigation of ferromagnetism and ferroelectricity in bismuth manganite, Phys. Rev. B 59 (13) (1999) 8759–8769.
[6] T. Kimura, T. Goto, H. Shintani, K. Ishizaka, T. Arima, Y. Tokura, Magnetic control of ferroelectric polarisation, Nature 426 (2003) 55–58.
[7] A.A. Belik, T. Yokosawa, K. Kimoto, Y. Matsui, E. Takayama-Muromachi, High-pressure synthesis and properties of solid solutions between $BiMnO_3$ and $BiScO_3$, Chem. Mater. 19 (7) (2007) 1679–1689.
[8] T. Atou, H. Chiba, K. Ohoyama, Y. Yamaguchi, Y. Syono, Structure determination of ferromagnetic perovskite $BiMnO_3$, J. Solid State Chem. 145 (2) (1999) 639–642.
[9] T. Yokosawa, A.A. Belik, T. Asaka, K. Kimoto, E. Takayama-Muromachi, Y. Matsui, Crystal symmetry of $BiMnO_3$: electron diffraction study, Phys. Rev. B 77 (2008) 024111.
[10] A. Sundaresan, R.V.K. Mangalam, A. Iyo, Y. Tanaka, C.N.R. Rao, Crucial role of oxygen stoichiometry in determining the structure and properties of $BiMnO_3$, J. Mater. Chem. 18 (2008) 2191–2193.
[11] A.A. Belik, S. Iikubo, T. Yokosawa, K. Kodama, N. Igawa, S. Shamoto, M. Azuma, M. Takano, K. Kimoto, Y. Matsui, E. Takayama-Muromachi, Origin of the monoclinic-to-monoclinic phase transition and evidence for the centrosymmetric crystal structure of $BiMnO_3$, J. Am. Chem. Soc. 129 (4) (2007) 971–977.
[12] A.A. Belik, T. Kolodiazhnyi, K. Kosuda, E. Takayama-Muromachi, Synthesis and properties of oxygen non-stoichiometric $BiMnO_3$, J. Mater. Chem. 19 (11) (2009) 1593–1600.
[13] A.A. Belik, H. Yusa, N. Hirao, Y. Oishi, E. Takayama-Muromachi, Peculiar high pressure behaviour of $BiMnO_3$, Inorg. Chem. 48 (3) (2009) 1000–1004.
[14] P. Toulemonde, C. Darie, C. Goujon, M. Legendre, T. Mendonca, M. Alvarez-Murga, V. Simonet, P. Bordet, P. Bouvier, J. Kreisel, M. Mezouar, Single crystal growth of $BiMnO_3$ under high pressure conditions, High Pressure Res. 29 (December (4)) (2009) 600–604.
[15] H.K. Mao, J. Xu, P.M. Bell, Calibration of the ruby pressure gauge to 800-kbar under quas-hydrostatic conditions, J Geophys. Res. Solid Earth Planets 91 (B5) (1986) 4673–4676.
[16] A.P. Hammersley, S.O. Svensson, M. Hanfland, A.N. Fitch, D. Hausemann, Two-dimensional detector software: from real detector to idealised image or two-theta scan, High Pressure Res. 14 (4–6) (1996) 235–248.
[17] Bruker AXS Ltd., TOPAS Software (Ver. 2.1), Bruker AXS Ltd., Coventry, UK, 2003.
[18] D.A. Fletcher, R.F. McMeeking, D. Parkin, The United Kingdom chemical database service, J. Chem. Inf. Comput. Sci. 36 (1996) 746–749.
[19] M. Thrall, R. Freer, C. Martin, F. Azough, B. Patterson, R.J. Cernik, An in situ study of the formation of multiferroic bismuth ferrite using high resolution synchrotron X-ray powder diffraction, J. Eur. Ceram. Soc. 28 (2008) 2567–2572.
[20] T. Atou, H. Faqir, M. Kikuchi, H. Chiba, Y. Syono, A new high pressure phase of $BiMnO_3$, Mater. Res. Bull. 33 (February (2)) (1998) 289–292.
[21] W. Paszkowicz, W. Szuszkiewicz, E. Dynowska, J.Z. Domagała, C. Lathe, Pressure distribution in a large-anvil pressure cell, J. Alloys Compd. 14 (2004) 94–98.